

Magnetic optical activity in intense laser fields. II. Forward scattering

S. Giraud-Cotton and V. P. Kaftandjian

Université de Provence, Centre St. Jérôme, 13397 Marseille Cedex 13, France

L. Klein

Department of Physics and Astronomy, Howard University, Washington, D.C. 20059

(Received 12 March 1985)

The theoretical formulation of the nonlinear optical activity is utilized to describe the signal intensity in forward scattering. For cases in which the ratio of the Rabi frequency of an isolated transition to its relaxation rate is less than one, a perturbation procedure in this parameter is presented. The successive terms in the resulting series are interpreted as higher-order coherences or induced multipole moments. Application is made to the hyperfine components of the sodium *D* transitions where experimental data is described by a third-order calculation. Good agreement is obtained without invoking an induced hexadecapole moment as was proposed originally.

I. INTRODUCTION

In our preceding article¹ the saturated magnetic rotation spectrum of a dilute gas was studied. That is, the nonlinear (in the radiation field) contribution to the change in intensity of laser light which has passed through a sample placed between crossed polarizer and analyzer in a longitudinal external magnetic field was investigated as a function of the incident laser frequency.

In the following, the same system is studied, but as a function of the external magnetic-field strength with a fixed laser frequency. It will be shown that this experimental arrangement which has been variously called forward scattering,² stimulated level crossing,³ or the forward Hanle effect⁴ has certain advantages not present in the more usual magnetic rotation spectroscopy.

Both of these methods are manifestation of nonlinear magnetic optical activity (MOA). That is, the intensity detected passing through the crossed analyzer is the combined result of the rotation of the plane of polarization [Faraday effect or magnetic circular birefringence (MCB)] and an induced ellipticity of the initial polarization [magnetic circular dichroism (MCD)]. This interpretation complements the usual forward-scattering formulation and permits an alternative physical picture of the effect. Thus, for example, the use of a crossed analyzer is seen to be simply a means of measuring the Faraday rotation and dichroism induced in the incident laser beam as it passes through the gyrotropic medium. Of course, this is the same thing as stating that the crossed analyzer rejects the incident beam and allows only the forward-scattering signal to pass (Corney *et al.*²), or that the angular intensity distribution of a scattered signal is modified by the presence of a magnetic field (although this latter interpretation of Feld *et al.*³ is independent of polarization).

In any case, the observed spectral profile yields important information on the spectroscopic parameters of the transition involved. In particular, a pressure-broadened line shape contains the effects of the interaction potential on the concerned levels. However, in cases for which the

Doppler broadening of the transition is important, this width dominates the magnetic rotation spectrum and information on the collisional contribution to the line shape is obscured. The light scattered in the forward direction, on the other hand, contains a component that is not Doppler shifted with respect to the incident radiation if velocity-changing collisions are ignored. This means that the signal detected in forward-scattering experiments will have a sub-Doppler contribution to the line profile and can be used to obtain information on the collision broadening parameters of the transition.

Sub-Doppler magnetic rotation spectroscopy can also be performed on this system with fixed magnetic-field strength, but a second counterpropagating laser is required to saturate the transition while the intensity of the probe beam is monitored as a function of its frequency.⁵ If the magnetic field is set to zero and a circularly polarized saturating laser is used, this technique, polarization spectroscopy, developed by Wieman and Hänsch,⁶ can also be used to measure sub-Doppler profiles. However, these methods require more sensitivity in the detection of the weak probe beam than do the forward-scattering experiments.⁷

The theory of magnetic optical activity developed in I will be used to analyze in detail the forward-scattering signal. That is, in varying the magnetic field, we vary the amount of MCD and MCB created in the system. This results in a modification of the signal detected through the crossed analyzer. This point of view is also equivalent to that in which the variation of the magnetic field is a means of inducing level crossings or a Hanle effect in the gas. Nevertheless, it is important to note that since the detection is through a crossed analyzer in the forward direction, a coherent effect is observed. Due to the random positions of the gas atoms it is evident that stimulated emission in other directions will be incoherent² and MOA will therefore not be observed as such. This is the principal difference between forward-scattering and the usual level-crossing experiments with a detector at right angles to the propagation direction of the incident radiation.

tion. The consequence of this difference is that there is linear (in the incident laser intensity) MOA in the forward direction and, hence, a linear contribution to the forward-scattering signal. This linear effect is, of course, absent in the spontaneous-emission Hanle-effect experiments since the signal is incoherent.

The linear effect has the full Doppler width, as is usual in unsaturated spectroscopy. However, with increasing laser power, higher-order contributions which saturate a particular velocity group appear. This pumping of specific velocities results in the appearance of narrow resonances superposed on the linear background. These are the stimulated-emission contributions that permit the possibility of sub-Doppler spectroscopy.

To illustrate the physical basis of the effect, consider the case of a transition from a level with angular momentum j_i to one with j_f . If the pumping laser frequency is within the Doppler width of the transition, it will saturate a selected velocity class. However, with a magnetic field splitting the $m_f = \pm 1$ Zeeman substrates of the upper level, different velocity classes will be saturated for $\Delta m = +1$ and $\Delta m = -1$ transitions. Since atoms pumped in these two transitions belong to different velocity groups, the pumping process is incoherent. However,

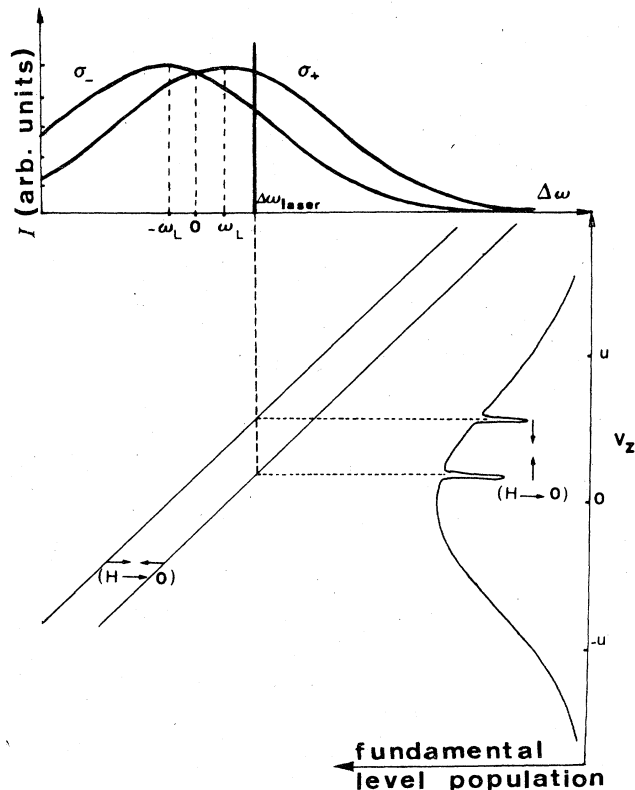


FIG. 1. Schematic interpretation of the stimulated Hanle effect on a $j_i=1 \rightarrow j_f=0$ transition. The hole burnings in the fundamental level ($j_i=1$) population for $m=+1$ and $m=-1$ states move in the direction indicated by the arrows when the intensity H of the magnetic field is turned to zero. They begin to overlap when their splitting is on the order of $\gamma_i(c/\omega)$ (where γ_i is the fundamental level half-width, in units of atomic velocity v_z) leading to cross coherence.

as the magnetic field is varied and the widths of the sub-levels begin to overlap, this level crossing creates a coherent quantum interference effect which is observed within the Doppler width. In Fig. 1 this description is illustrated for the case of a $0 \rightarrow 1$ transition. Note that only the intensity of the stimulated Hanle effect depends on the laser detuning. This dependence is the same as in the spontaneous-emission effect.

From this we see that the saturated forward-scattering signal depends on the Landé factors and coherences of the two states coupled by the laser, unlike spontaneous-emission level-crossing signals which depend only on those quantities for the excited state. In addition, since the forward scattering through the crossed analyzer must vanish in zero magnetic field (where the system becomes isotropic), these are null observations with much greater sensitivity than the usual absorption or emission spectroscopy experiments.

Finally, we note that forward scattering can also be observed using Stark splittings instead of the Zeeman effect discussed above. Experiments of this type on CH_3OH in an electric field have been recently performed by Inguscio *et al.*⁸ with results analogous to those discussed here.

In the next sections the method of calculation outlined in I will be reviewed and applied to the case of forward scattering resonant with the D lines of Na. Comparison with the experimental studies of Gawlik *et al.*⁷ is given along with an interpretation in terms of the multipole moments induced by the coherences. The interpretation is analogous, but not identical, to that which has been developed for the spontaneous Hanle effect by Ducloy,⁹ and these differences will be discussed.

II. FORWARD SCATTERING

As explained above, the calculation of the nonlinear optical activity developed in I will be used to obtain expressions for the signal scattered in the forward direction as a function of the external longitudinal magnetic field. The signal observed in these experiments is the intensity of a monochromatic wave which passes through crossed polarizer and analyzer. The left and right circularly polarized components of the radiation become dephased because of the asymmetry induced by the magnetic field. This dephasing results in a Faraday rotation per unit length Θ/L and a corresponding ellipticity Ψ/L . The observed signal can be written in terms of these quantities as

$$I = I_0(\sin^2\Theta + \sinh^2\Psi) \times \exp[(-2\pi\omega L/c)\text{Im}(\chi_r + \chi_l)], \quad (1)$$

where χ_r (χ_l) is the right (left) circularly polarized component of the electrical susceptibility of the medium. The complex Faraday effect in terms of these susceptibilities is

$$\Theta + i\Psi = (\pi\omega L/c)(\chi_r - \chi_l). \quad (2)$$

For dilute gases, the imaginary part of the susceptibility is small as is the left-right difference of the susceptibilities. Thus, for path lengths not too large, the fraction of the intensity passing through the analyzer is proportional to simply $\Theta^2 + \Psi^2$, the sum of the squares of the rotation

angle and the ellipticity.

Since stimulated zero-field level crossings are to be observed, the case from I for weak magnetic fields and for which the laser is quasiresonant with an isolated transition of the atomic system will be used.

A complete discussion of the method of calculation of the nonlinear contribution to χ_r (χ_f) under the appropriate condition for magnetic optical activity has been given in I. The method used was based on an iterative solution to a Dyson equation for the line-shape Green's function written as an operator in the Liouville space of the system states and a space of harmonic numbers of the external laser field.¹⁰ The iteration produces a power-series solution in the laser intensity and is capable of being summed to all orders in a dressed-atom type of theory.¹¹ The all-orders solution adapted to the resonant, weak-field, Doppler-broadened case is discussed in I and completely presented in Ref. 12. This solution (which is exact within the rotating-wave approximation) displays power broadening and shift and contains the complete features of the

Lamb-dip-type saturation phenomena of Doppler-broadened transitions. For laser intensities and transitions such that the Rabi frequency is less than the relaxation width of the transition, these effects can be approximated by a finite-series solution.

The lowest-order contribution is, as mentioned above, the linear Faraday effect and, of course, displays no intensity-dependent saturation effects. The expression for this term, given in I, will be rewritten below in order to recall the notation. The field will be taken to be weak enough so that the Zeeman splittings of the levels involved in the transition considered can be assumed to be less than their widths. This ensures that the collisional mixing of the Zeeman components can be neglected so that the relaxation matrix is diagonal.¹³ The angle of rotation per unit length in first approximation, $\Theta^{(1)}/L$, and the corresponding ellipticity, $\Psi^{(1)}/L$, for an isolated Doppler-broadened transition $i \rightarrow f$ of frequency ω_{fi} in a gas of N_A atoms in a volume V and in a longitudinal magnetic field with Larmor frequency ω_L are

$$(\Theta^{(1)} + i\Psi^{(1)})/L = -(N_A/V)(\rho_i - \rho_f) \frac{2\pi |d_{fi}|^2 \omega \omega_L}{3\hbar c \omega_D} [1 - z_{fi} Z(z_{fi})] \left[g_i + g_f + (g_i - g_f) \frac{j_i(j_i + 1) - j_f(j_f + 1)}{2} \right], \quad (3)$$

where ω_D is the Doppler width of the transition, $\omega_D = (2kT/m)^{1/2} \omega/c$, ρ_i and ρ_f are the equilibrium populations of the levels with Landé g factors g_i and g_f , and d_{fi} is the dipole-moment reduced matrix element of the transition. $Z(z_{fi})$ is the plasma dispersion function (see, for instance, Ref. 14) with the argument

$$z_{fi} = (1/\omega_D)(\omega - \omega_{fi} + \langle \Pi_{fi}^{(1)} \rangle).$$

In the limit of a very small detuning, $\Delta\omega = \omega - \omega_{fi}$, $Z(z_{fi}) \rightarrow i\sqrt{\pi}$ and Eq. (3) leads to

$$\Theta^{(1)}/L = -(N_A/V)(\rho_i - \rho_f) \frac{2\pi |d_{fi}|^2 \omega \omega_L}{3\hbar c \omega_D} \left[g_i + g_f + (g_i - g_f) \frac{j_i(j_i + 1) - j_f(j_f + 1)}{2} \right]. \quad (4)$$

The ellipticity $\Psi^{(1)}/L$ vanishes in this limit. We note, in addition, that the signal detected in the small-rotation limit is a quadratic function of ω_L . Thus, as expected, whenever the transition width is dominated by the Doppler effect, so is the linear contribution to the Faraday rotation.

The next contribution, the third-order term, which contains the lowest-order saturation effects, will display the sub-Doppler collisional width parameter. Again assuming a diagonal relaxation matrix for an isolated Doppler-broadened $j_i \rightarrow j_f$ transition, we have

$$\begin{aligned} \Theta^{(3)}/L = & (N_A/V)(\rho_i - \rho_f) \frac{\pi^{3/2} |d_{fi}|^2 \omega \beta_R^2}{2\hbar c \omega_D \gamma_{fi}^2} \exp(-\Delta\omega^2/\omega_D^2) \\ & \times \left[\frac{x_f}{x_f^2 + 1} \left[\Gamma_i^{-1} + \frac{2 + \Gamma_f}{4x_f^2 + \Gamma_f^2} \right] \sum_{m_i} \begin{bmatrix} j_f & 1 & j_i \\ -(m_i + 1) & 1 & m_i \end{bmatrix}^2 \begin{bmatrix} j_f & 1 & j_i \\ -(m_i - 1) & -1 & m_i \end{bmatrix}^2 \right. \\ & \left. + \frac{x_i}{x_i^2 + 1} \left[\Gamma_f^{-1} + \frac{2 + \Gamma_i}{4x_i^2 + \Gamma_i^2} \right] \sum_{m_i} \begin{bmatrix} j_f & 1 & j_i \\ -(m_i - 1) & 1 & m_i \end{bmatrix}^2 \begin{bmatrix} j_f & 1 & j_i \\ -(m_i - 1) & 1 & (m_i - 2) \end{bmatrix}^2 \right], \quad (5) \end{aligned}$$

where $x_a = g_a \omega_L / \gamma_{fi}$, $\Gamma_a = \gamma_a / \gamma_{fi}$ are the dimensionless Larmor frequency and the relaxation parameter of the a level. The square of the reduced Rabi frequency, $(\beta_R / \gamma_{fi})^2 = |d_{fi} E_L|^2 / \hbar^2 \gamma_{fi}^2$, is the expansion parameter which orders the terms in the iteration series for the nonlinear contributions. The level relaxation, orientation, and alignment parameters are all taken to be the same in Eq.

(5).

The contribution of Eq. (5) to the Faraday rotation can be seen to be composed of two dispersion functions of the reduced Larmor frequency. This means that the small-angle third-order contribution to the forward scattering [the square of Eq. (5)] has a narrow dip about $\omega_L = 0$. The width of that dip is $\Gamma_i/2$, and its amplitude is related

to the level relaxation parameter as well. On the other hand, the $\Delta\omega$ dependence with fixed ω_L , which is the magnetic rotation spectrum, is a Doppler-broadened Gaussian function with width ω_D .

This shows explicitly that the third-order forward-scattering contribution, unlike that of the magnetic rotation spectrum, contains a sub-Doppler component. It can also be seen that as long as the laser is tuned to within the Doppler width of the transition, the amplitude of the forward-scattering signal is only weakly dependent on the detuning $\Delta\omega_{fi}$.

Finally, it should be noted that the weak-rotation limit of Eq. (1) can be written, for this case,

$$I/I_0 \sim (\Theta^{(1)} + \Theta^{(3)})^2 \quad (6)$$

to third order. Since $\Theta^{(1)}$ is linear in ω_L and is independent of the laser intensity and $\Theta^{(3)}$ has a dispersion shape in ω_L and has a linear dependence on laser intensity, it is clear that the shape of the resonances observed in forward scattering will be a sensitive function of the laser intensity even though the third-order calculation contains no power

broadening of the transition. In addition to this intensity-dependent shape effect, the amplitude of the signal has contributions proportional to the first and second powers of the laser intensity to this order of approximation.^{15,16}

The role of different dipole transition widths $\gamma_{fi}(1)$ and level- a relaxation, alignment, and orientation rates $\gamma_a(0)$, $\gamma_a(1)$, and $\gamma_a(2)$ can be made explicit in the simple case of a transition with $j_i = j_f$ or in one with a normal Zeeman effect. In both these cases the Landé g factor of the two levels is the same and we have, with the reduced quantity $x = x_i = x_f = \omega_L g / \gamma_{fi}(1)$,

$$\Theta^{(3)}/L = (N_A/V)(\rho_i - \rho_f) \frac{\pi^{3/2} |d_{fi}|^2 \omega \beta_R^2}{\hbar c \omega_D} \frac{x}{\gamma_{fi}^2 x^2 + 1} \times \exp(-\Delta\omega^2/\omega_D^2) D, \quad (7)$$

$$\Psi^{(3)}/L = 0,$$

where

$$D = \sum_{K=0}^2 \left\{ \frac{(K-2)(4K-1)}{6} \left[\begin{matrix} K & 1 & 1 \\ j_f & j_i & j_i \end{matrix} \right]^2 \Gamma_i^{-1}(K) + \begin{matrix} K & 1 & 1 \\ j_i & j_f & j_f \end{matrix} \right]^2 \Gamma_f^{-1}(K) \right\} + \frac{K(K-1)}{2} \left[\begin{matrix} K & 1 & 1 \\ j_f & j_i & j_i \end{matrix} \right]^2 \left[\frac{\Gamma_i^{-1}(K)}{6} + \frac{2 + \Gamma_i(K)}{4x^2 + \Gamma_i^2(K)} \right] + \left[\begin{matrix} K & 1 & 1 \\ j_i & j_f & j_f \end{matrix} \right]^2 \left[\frac{\Gamma_f^{-1}(K)}{6} + \frac{2 + \Gamma_f(K)}{4x^2 + \Gamma_f^2(K)} \right] \right\}. \quad (8)$$

From this result it is obvious that in the third-order term no Zeeman coherences higher than second order arise. These coherences which can be interpreted as induced quadrupole moments dominate the nonlinear Faraday effect whenever the Rabi frequency is less than the relaxation parameter. The situation is not the same for the spontaneous Hanle effect where, under the same conditions, interferences between the levels may cause cancellation so that the fifth-order coherences may dominate.⁹ These induced hexadecapole moments have been observed in Hanle-effect experiments on neon by Ducloy *et al.*¹⁷ In Sec. III we shall show that similar experiments performed in forward scattering on Na by Gawlik *et al.*⁷ and originally interpreted in the same manner can be described in terms of the lower-order induced quadrupole moment.

III. APPLICATION TO SODIUM D TRANSITIONS

The forward-scattering intensity, discussed in Sec. II, will now be calculated explicitly to third order for the sodium D lines. The hyperfine structure of these transitions (from Ref. 18) is displayed in Fig. 2. The parameters used in the calculation are those appropriate for comparison with the experimental observations of Gawlik

et al.,⁷ that is, a pressure of 5×10^{-6} Torr of sodium and a temperature of 160°C . These conditions imply a collisional contribution small with respect to the natural width, $\gamma_{fi} = (\gamma_i + \gamma_f)/2 = 4.98$ MHz where $\gamma_f = 9.65$ MHz and $\gamma_i = 0.3$ MHz (due to transit time through the beam diameter, 0.18 cm), and imply also a Doppler width, $\omega_D = 950$ MHz, which is much larger than the natural width. The laser intensity, in the range 0.05–0.15 mW, distributed over 50 MHz, gives a reduced Rabi frequency in the range 0.13–0.23, small enough so that the third-

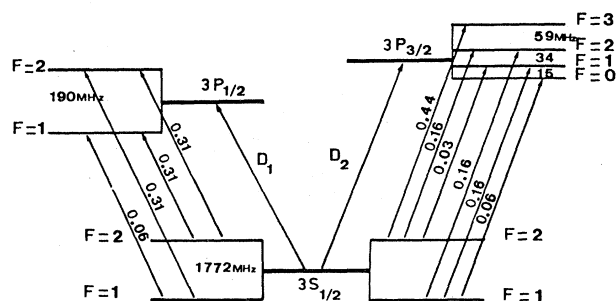


FIG. 2. Hyperfine structure of the D_1 and D_2 transitions of Na.

order calculation outlined above should be sufficient. The center frequency is tuned to within the Doppler width of each line considered.

Because the frequency spread of the incident laser in the experiments of Gawlik *et al.* was of the order of the hyperfine splitting of the upper states, the contributions from the hyperfine transitions $F_i \rightarrow F_f$ with the same F_i are added together to obtain the Faraday rotation.

To illustrate the calculation, the third-order Faraday rotation is displayed in Fig. 3 for one set of hyperfine transitions for each D line. The curves have the dispersion shape described by Eq. (5).

The forward-scattered intensity, calculated from Eq. (1), is given in Fig. 4, for each group of distinct hyperfine

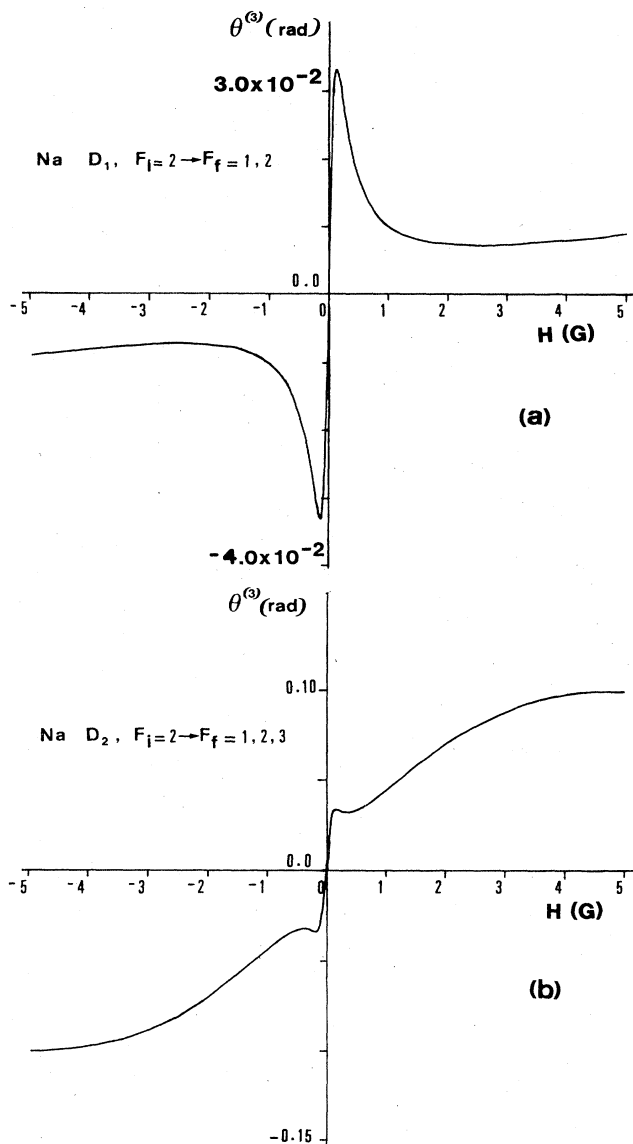


FIG. 3. Third-order contribution to the Faraday rotation from (a) the group of D_1 transitions originating from the $^2S_{1/2, F=2}$ level and (b) the group of D_2 transitions originating from the $^2S_{1/2, F=2}$ level. The laser power is $P_0=0.24$ mW, the beam radius is $R=0.15$ cm, and the path length is $L=5$ cm.

transitions; in 4(a) and 4(b) are those arising from the $^2S_{1/2, F=1}$ and $^2S_{1/2, F=2}$ levels for the D_1 line and in 4(c) and 4(d) are the analogous transitions for the D_2 line. Note that the signal for the D_1 and D_2 lines arising from the $^2S_{1/2, F=1}$ level is predicted to be more than two orders of magnitude weaker than the other component of these lines. This agrees with the observation made by Gawlik *et al.*⁷ that this component was too weak to be measured. Since, in addition, it is separated by about 1600 MHz from the other component for each line, which is about twice the Doppler width, it can be neglected in analyzing the experimental results centered about the other hyperfine component. Note also, that in the range of laser intensities used, the shape of the scattered intensity is greatly altered by increasing the reduced Rabi frequency. In Figs. 5(a) and 5(b), which reproduce the two theoretical curves from Figs. 4(b) and 4(d), we have displayed the experimental curves of Ref. 7, normalized to the intensity of the first resonance, for comparison with our theoretical predictions for low magnetic-field strengths. Since Eq. (5) has been calculated for a monochromatic laser source, we have not attempted a quantitative fit with the experimental data, since this was taken using a laser with a 50-MHz width (this would be a simple but meaningless exercise). Instead, we insist upon the excellent qualitative agreement of the third-order theory and note that no fifth-order contributions are necessary at these power levels. This corrects what we believe to be a misinterpretation^{4,15,16} of their experimental results by the authors of Ref. 7.

For larger magnetic fields, the experimental curves of Ref. 7 contain structure at 15 and 27 G which is probably due to the hyperfine level crossings that occur at these points. The theory presented in I contains these effects in principle, but they have been neglected in Eq. (5), in the isolated line approximation. For this reason, the theoretical curves have been plotted only in the restricted range of 5 G about the zero-field level crossing.

Finally, the independence of the structure on detuning within the Doppler width of the transition, predicted by Eq. (5), has been also studied experimentally by Gawlik *et al.*,⁷ by using a piezoelectric sweep of the dye laser. This "quasi-broad-band-excitation" method produced the same structure as was observed by excitation with the fixed laser frequency. The dependence on the reduced Rabi frequency of the sub-Doppler third-order terms was also tested by adding 6 Torr of Ne buffer gas to increase greatly the dipole relaxation parameter γ_{fi} and, hence, reduce β_R . The resulting forward-scattering signal then displays the parabolic first-order contribution unmodified by the now small third-order resonance, as expected.

In conclusion, it is to be noted that the nonlinear resonant Faraday effect as measured in forward-scattering experiments can be an important tool for the determination of level lifetimes of both levels involved in an isolated electric-dipole transition. This depends, however, on the existence of a sufficient difference in the characteristic parameters such as Landé factors, lifetimes, etc. This means that it should be an especially interesting method whenever one of the levels is a true ground state (or a metastable state). These states are, of course, inaccessible to study by the spontaneous-emission Hanle effect. As can be seen by

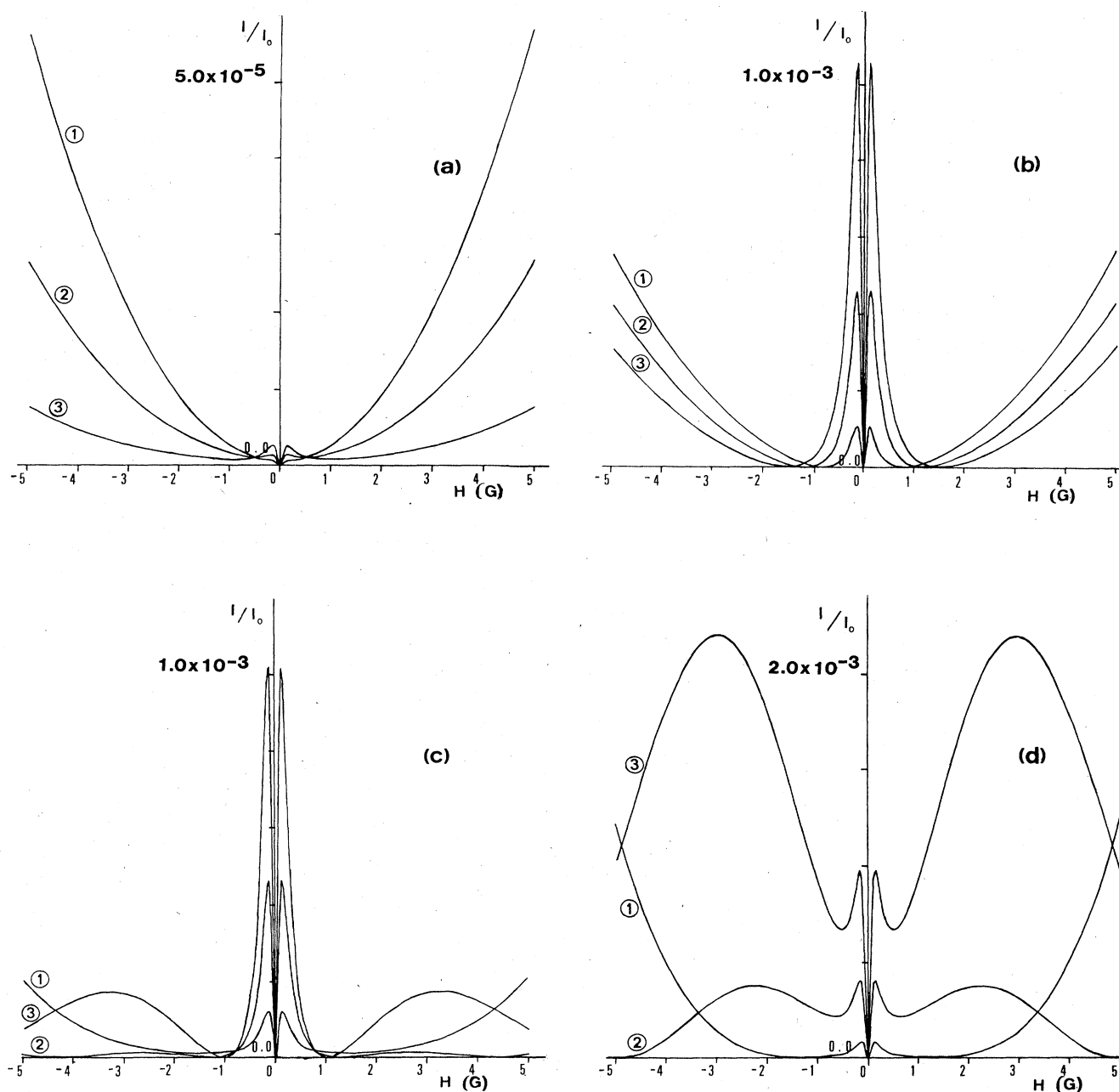


FIG. 4. Theoretical forward scattering (intensity through crossed polarizer and analyzer) as a function of the external longitudinal magnetic field for the indicated group of transitions (a) $D_1, F_i=1, F_f=1,2$; (b) $D_1, F_i=2, F_f=1,2$; (c) $D_2, F_i=1, F_f=0,1,2$; (d) $D_2, F_i=2, F_f=1,2,3$ for different values of the laser power, $P_0=K \times 0.08$ mW, $K=1, 2$, or 3 , is indicated in circles. The beam radius is 0.15 cm and the path length is $L=5$ cm as above.

reference to Fig. 4, for magnetic fields of less than one gauss the shape of the forward-scattering signal is closely linked to the rate of decay of population and induced quadrupole moments described in Eq. (5). For the laser intensity used above, it seems that it is unnecessary to invoke fifth-order terms which contain the induced hexadecapole moment as was suggested in Ref. 7. Nevertheless, the theory presented here is a perturbative series in β_R^2 , and with increasing laser intensity, higher-order terms

will eventually make a small contribution. When power broadening becomes significant, however, the entire perturbative approach (and the interpretation in terms of successively important higher-order coherences) must be abandoned and a nonperturbative technique used. Formulas for calculating closed-form solutions for isolated transitions in the arbitrary angular momentum case within the rotating-wave approximation are given by Giraud-Cotton.¹²

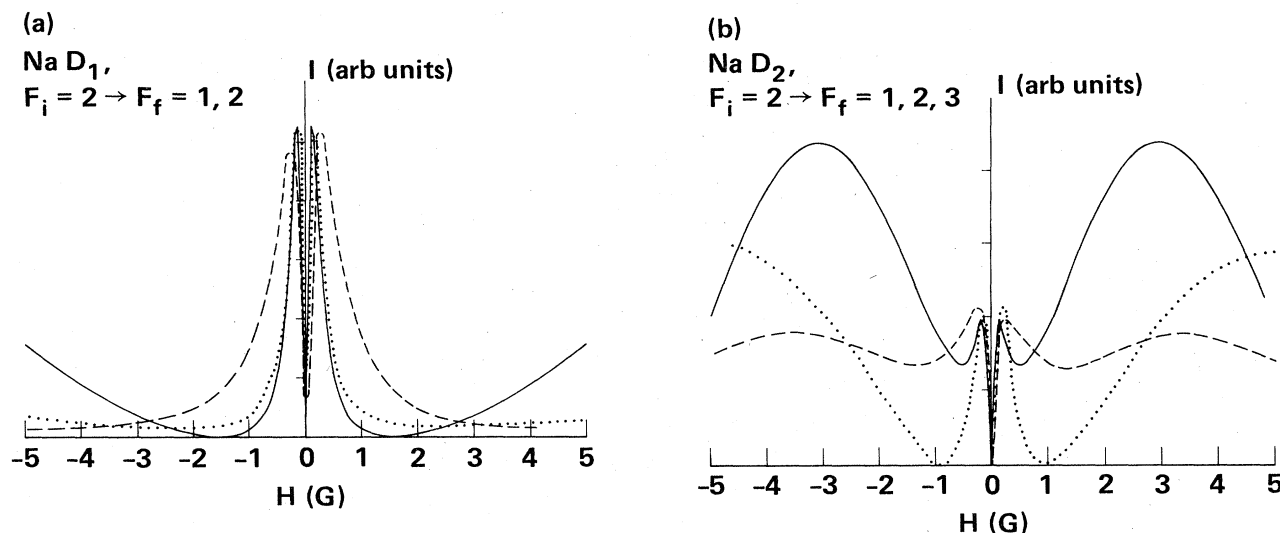


FIG. 5. Theoretical third-order forward-scattering calculation (solid line) using the same parameters as in Figs. 3 and 4 and a laser power of 0.24 mW. Comparison with two experimental patterns (dashed lines) recorded at different laser power levels from Gawlik *et al.* (Ref. 7) for each of two groups of transitions. (a) $\text{Na } D_1$: \cdots , 0.5 mW; $---$, 3 mW. (b) $\text{Na } D_2$: \cdots , 0.3 mW; $---$, 2.5 mW.

ACKNOWLEDGMENTS

S. G.-C. and V. P. K. are part of the "Laboratoire Physique des Interactions Ioniques et Moléculaires," Equipe de Recherche associée au Centre National de la Recherche

Scientifique, No. 07.898, at the Université de Provence. Part of this research was performed while L.K. was a visiting professor at the Université de Provence. This work was supported in part by U.S. National Aeronautic and Space Administration Grant No. NAGW-545 through Howard University.

- ¹S. Giraud-Cotton, V. P. Kaftandjian, and L. Klein, preceding paper, *Phys. Rev. A* **32**, 2211 (1985) (hereafter referred to as I).
- ²A. Corney, B. Kibble, and G. Series, *Proc. R. Soc. London, Ser. A* **293**, 70 (1966).
- ³M. Feld, A. Sanchez, A. Javan, and B. Feldman, *Colloq. Int. C.N.R.S.* **217**, 87 (1973).
- ⁴S. Giraud-Cotton, V. P. Kaftandjian, and L. Klein, *Phys. Lett.* **88A**, 453 (1982).
- ⁵S. Giraud-Cotton, V. P. Kaftandjian, and B. Talin, *J. Phys. (Paris) Lett.* **41**, L-591 (1980).
- ⁶C. Wiemann and T. Hänsch, *Phys. Rev. Lett.* **36**, 1170 (1976).
- ⁷W. Gawlik, J. Kowalski, R. Neumann, and F. Träger, *Opt. Commun.* **12**, 400 (1974).
- ⁸M. Inguscio, A. Moretti, and F. Strumia, *IEEE J. Quantum Electron* **QE-16**, 955 (1980).
- ⁹M. Ducloy, *Phys. Rev. A* **8**, 1844 (1973); **9**, 1319 (1974).
- ¹⁰A. Ben-Reuven and L. Klein, *Phys. Rev. A* **4**, 753 (1971).
- ¹¹L. Klein, M. Giraud, and A. Ben-Reuven, *Phys. Rev. A* **16**, 289 (1977).
- ¹²S. Giraud-Cotton, Thèse de Doctorat d'Etat, Université de Provence, Marseille, 1982.
- ¹³S. Giraud-Cotton, M. Giraud, and L. Klein, *Chem. Phys. Lett.* **32**, 317 (1975).
- ¹⁴A. Lindgard and S. Nielsen, *At. Data Nucl. Data Tables* **19**, 571 (1977).
- ¹⁵W. Gawlik, *Phys. Lett.* **89A**, 278 (1982).
- ¹⁶S. Giraud-Cotton, V. P. Kaftandjian, and L. Klein, *Phys. Lett.* **90A**, 393 (1982).
- ¹⁷M. Ducloy, M. Gorza, and B. Decomps, *Opt. Commun.* **8**, 21 (1973).
- ¹⁸J. Bjorkholm and P. Liao, *Phys. Rev. A* **14**, 751 (1976).